

Received January 11, 2020, accepted February 1, 2020, date of publication February 5, 2020, date of current version February 13, 2020.

Digital Object Identifier 10.1109/ACCESS.2020.2971860

# Wideband Circularly Polarized Magneto-Electric Dipole $1 \times 2$ Antenna Array for Millimeter-Wave Applications

YING-FANG WANG<sup>ID</sup>, BIAN WU<sup>ID</sup>, (Member, IEEE), NAN ZHANG<sup>ID</sup>,  
YU-TONG ZHAO<sup>ID</sup>, AND TAO SU<sup>ID</sup>

National Key Laboratory of Antennas and Microwave Technology, Xidian University, Xi'an 710071, China

Corresponding author: Bian Wu (bwu@mail.xidian.edu.cn)

This work was supported in part by the National Natural Science Foundation of China (NSFC) under Project 61771360 and Project U19A2055, in part by the Key Industry Chain Project of Shaanxi Province under Grant 2018ZDCXL-GY-08-03-01, in part by the Key Laboratory Foundation under Grant 6142216180104, and in part by the Fundamental Research Funds for the Central Universities.

**ABSTRACT** A novel wideband circularly polarized (CP) magneto-electric (ME) dipole  $1 \times 2$  antenna array for millimeter-wave applications is presented in this paper. The magneto-electric dipole of a single radiator is designed by combining a pair of loaded short-circuited metallic patches acting as electric dipole with a bowtie-shape aperture and a pair of vertical metallic posts functioned as a magnetic dipole. The pair of metallic patches is fed by the bowtie-shape aperture etched on the top surface of shorted-end substrate integrated waveguide (SIW). By chamfering and adding perturbation on each rectangular patch, the proposed ME dipole antenna realizes circular polarization radiation. Measured results show that the proposed single radiator has an impedance bandwidth of 27.1% (24.29 to 31.9GHz) for  $S_{11} < -10\text{dB}$ , an axial-ratio (AR) bandwidth of 9.7% (27.4 to 30.2GHz) for  $\text{AR} < 3\text{dB}$ , and a stable gain of 7dBic. In order to extend AR bandwidth, the array antenna is implemented in a  $1 \times 2$  arrangement and fed by a complementary SIW power distribution phase shifter. The proposed antenna has a simple structure and can be realized by PCB process, which is very convenient for mass production. Measured results demonstrate that the proposed  $1 \times 2$  antenna array has a wide impedance bandwidth of 25% for  $S_{11} < -10\text{dB}$ , a stable gain of 10dBic and an axial-ratio bandwidth of 24.7% for  $\text{AR} < 3\text{dB}$ , which is 2.4 times higher than the 3-dB AR bandwidth of a single radiator.

**INDEX TERMS** Circularly polarized, magneto-electric dipole, wideband, perturbation, chamfer.

## I. INTRODUCTION

Circularly polarized antennas have been widely applied in satellite communication, mobile communication and wireless power transmission systems, due to their good performance of reducing the bad influence of interference from multi-path and mismatch of polarization [1]–[5]. The basic implementation method of a CP antenna is radiating two kind of field components, of which the amplitude is same and the phase has a difference of  $90^\circ$  [6]. In the past years, some of circularly polarized antennas have been reported [7], [8]. The slotted cavity linearly polarized antenna array, which uses the SIW technology and has the high-order cavity modes, could become a CP antenna array by adding rotated dipole array [9]. Due to the polarization conversion metasurface beneath the dipole antenna, the CP radiation could be realized

by the radiated wave and the reflected wave, of which the amplitude is same and the phase has a difference of  $90^\circ$  [10]. The four-element CP microstrip antenna array with a feed network, which uses the technique of sequentially rotated series-parallel stub, has been studied in [11]. In [12], a CP Fabry-Perot cavity antenna is introduced, which can control the phase and magnitude response of reflection and transmission coefficient independently by employing double-sided partially reflective surface. A CP antenna array, which employs aperture-coupled two-arm spiral antenna as its radiating element and is excited by the substrate integrated cavity, has been proposed in [13].

However, those antennas mentioned above suffer from a narrow AR bandwidth. Many methods including stacked patch, adding parasitic patch and co-design of feeding network, are used to broaden the AR bandwidth. A CP aperture-fed stacked patch antenna is studied in [14]. The antenna includes four parasitic patches in four

The associate editor coordinating the review of this manuscript and approving it for publication was Yejun He<sup>ID</sup>.

different layers, and each parasitic patch is rotated by the angle of  $30^\circ$ , which could broaden the AR bandwidth. However, it has a high profile and the precise alignment is required for those radiators. Due to four parasitic strips around the patch, the corner-truncated patch antenna has an AR bandwidth of 24% in [15]. A capacitive-coupled CP microstrip antenna fed by the probe is introduced [16]. The antenna has wide impedance bandwidth and AR bandwidth by setting four coplanar parasitic ring slot patches around the circular patch. The microstrip CP antenna fed by a modified L-shaped probe, has a wide AR bandwidth [17]. A CP patch antenna array is designed with a stripline sequential rotation feeding scheme [18], which is used for achieving wide axial-ratio bandwidth. However, the AR bandwidth is still narrow and those antennas may be not suitable for nowadays wideband communication systems. There are other antennas with wide bandwidth. The  $8 \times 8$  CP antenna array with a complex feed network has a wide AR bandwidth [19]. However, in order to get the good radiation performance and impedance matching, it is necessary to tune the dimensions of the antenna element, and it's difficult obviously. With the tapered dielectric rod, the CP complementary source antenna has a wide 3-dB AR bandwidth and high gain [20]. However, this approach of adding tapered dielectric rod is not universal. When adopting this approach for a high frequency bandwidth, the dielectric substrates will be thinner, and it will lead to a lower structural rigidity. A wideband circular polarization antenna excited by microstrip lines is described in [21]. However, in order to reduce the back radiations, the electromagnetic bandgap layer is necessary. And the antenna is not suitable for a high frequency bandwidth. The circularly polarized antenna array excited by gap waveguide is described in [22], [23], for which the precise fabrication process is necessary for the complex feed network.

In this paper, a novel wideband CP magneto-electric dipole antenna for millimeter-wave applications is designed. The proposed antenna consists of a bowtie-shape aperture and a pair of vertical metallic posts, which are functioned as the magnetic dipole, and a pair of metallic patches, which are short-circuited by a pair of vertical metallic posts and can realize electric dipole radiation. By chamfering and adding perturbation on the rectangular patches, the proposed antenna realizes CP radiation. The structure of the proposed antenna is very simple. In order to extend AR bandwidth, its array antennas are implemented in a  $1 \times 2$  arrangement and fed by a complementary SIW power distribution phase shifter. The proposed  $1 \times 2$  antenna array has a good performance of wide AR bandwidth and good polarization isolation. Moreover, the radiation pattern of the xoz plane is very similar with the radiation pattern of the yoz plane.

**II. ANTENNA ELEMENT DESCRIPTION**  
**A. GEOMETRY OF ANTENNA ELEMENT**

The geometry of the proposed wideband CP magneto-electric dipole antenna is shown in Fig.1. The proposed antenna comprises two layers of Rogers5880 substrates, of which

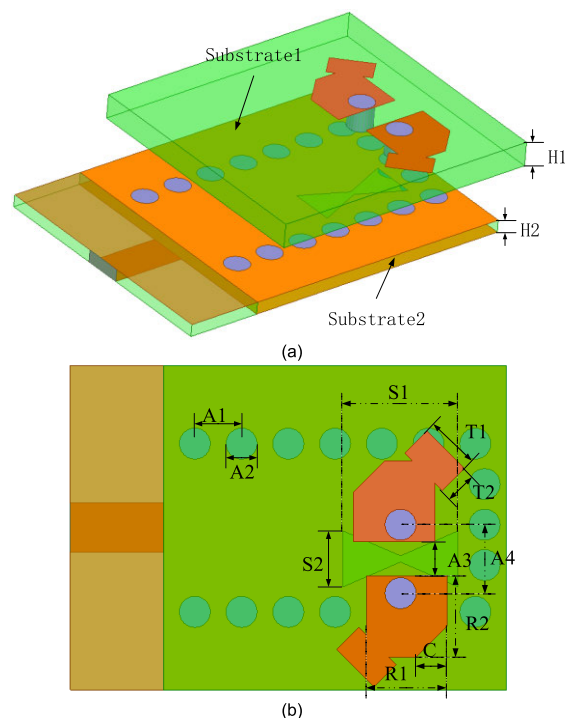


**FIGURE 1. Geometry of the proposed antenna. (a) 3D view. (b) Top view.**

**TABLE 1. Dimensional parameters of the proposed antenna.**

Parameter	A1	A2	A3	A4	S1	S2	T1
Value(mm)	1.5	1	0.55	2.2	3.7	1.8	1
Parameter	T2	R1	R2	C	H1	H2	
Value(mm)	1.7	2.6	2.6	1	1	0.508	

the relative dielectric constant is 2.2 and the loss tangent is 0.0009. A short-ended section of SIW is designed in Substrate 2, which has a thickness of 0.508mm, to feed the antenna. Blind metallic posts with diameter of 1mm are used as the metallic post wall of the substrate integrated waveguide cavity, and the center of neighboring metallic posts has the same distance of 1.5mm. A bowtie-shape aperture is etched on the middle metallic layer, which is also used as the top metallic surface of the proposed substrate integrated waveguide cavity. The center of the bowtie-shape aperture has the distance of around quarter-wavelength at the center frequency with the end metallic post wall of the substrate integrated waveguide cavity. All radiation parts are built in Substrate 1, which is composed of two horizontal metallic patches with chamfering and perturbation, and two vertical metallic posts. Vertical metallic posts are used to connect two horizontal metallic patches with the middle metallic layer. The thickness of Substrate 1 is around quarter-wavelength at the center frequency. Detailed dimensions of the antenna are given in Table 1.

The electromagnetic energy is coupled to the metallic patches through the bowtie-shape aperture etched on the middle metallic layer. The bowtie-shape aperture and a pair of vertical metallic posts are used to realize magnetic

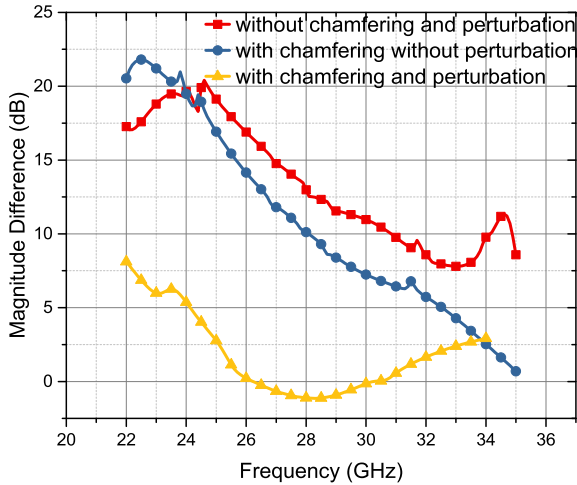


**FIGURE 2.** Simulated magnitude difference of the proposed antenna with and without chamfering or perturbation.

dipole radiation. A pair of loaded short-circuited metallic patches acts as an electric dipole. The electric dipole can be compensated by the magnetic dipole which is perpendicular to the electric dipole. When the electric dipole and the magnetic dipole are fed by proper amplitudes and phases, good characteristics such as low back radiation, stable antenna gain and symmetric E-plane and H-plane pattern can be achieved. By chamfering and adding perturbation on rectangular patches, the two orthogonal degenerate modes are separated. By adjusting the magnitude of chamfering and perturbation, the phase of one mode is  $45^\circ$  ahead and the phase of the other mode is  $45^\circ$  behind, which would produce a phase difference of  $90^\circ$  and be satisfied with the phase difference condition. Therefore, the proposed antenna may be realizing circular polarization radiation.

The simulated result is shown in Fig.2 to illustrate the role of chamfering and perturbation on the magnitude difference. Over the operating band, the magnitude difference is large when rectangular patches don't have chamfering and perturbation, which means the electric field vector basically only has the vertical direction component, and the antenna is a linearly polarized antenna. The magnitude difference decreases by 2-3dB when rectangular patches have chamfering but don't have perturbation, which means the electric field vector has a horizontal component in addition to the vertical direction component. The magnitude difference is almost 0 dB, when rectangular patches have both chamfering and perturbation, which means the vertical direction component and the horizontal component of the electric field vector are substantially equal, and the antenna may become a circularly polarized antenna.

In order to illustrate the operating mechanism of the proposed wideband circularly polarized magneto-electric dipole antenna, as shown in Fig.3, the current distribution at different times  $t = 0, T/4, T/2$  and  $3T/4$  is simulated, where  $T$  is the period of oscillation when operating frequency is 28GHz. It is seen that, at time  $t = 0$ , the current on the surface of the

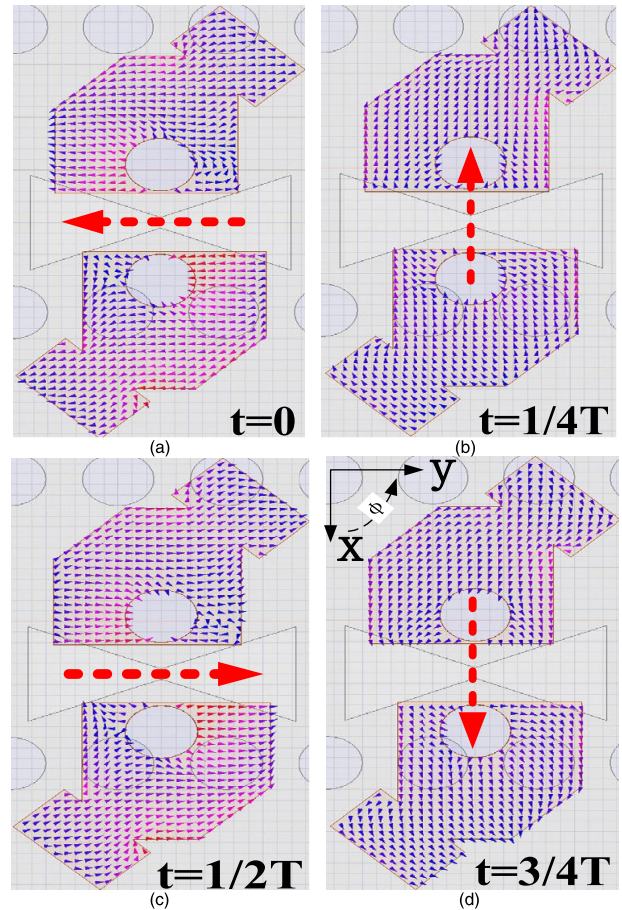


**FIGURE 3.** Current distribution of the proposed antenna at 28 GHz. (a)  $t = 0$ , (b)  $t = T/4$ , (c)  $t = T/2$ , (d)  $t = 3T/4$ .

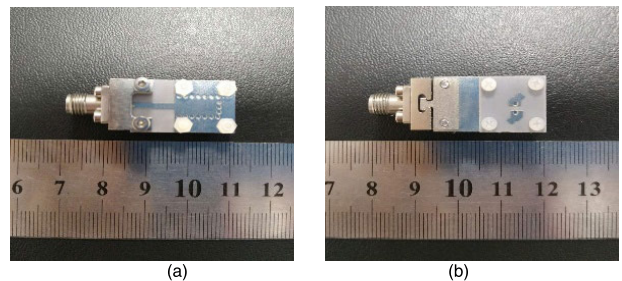


**FIGURE 4.** Fabricated prototype of the proposed antenna. (a) Top view, (b) bottom view.

proposed antenna flows along the direction of  $\varphi = -\pi/2$ . As  $t = T/4$ , the antenna's surface current flows along the direction of  $\varphi = \pi$ . As  $t = T/2$ , the surface current flows along the direction of  $\varphi = \pi/2$ . As  $t = 3T/4$ , the surface current flows along the direction of  $\varphi = 0$ . With the time varies, the current on the antenna's surface rotates in the clockwise direction. Therefore, the proposed magneto-electric dipole antenna can generate a CP radiation, which is left-hand CP wave.

**B. EXPERIMENTAL RESULTS OF ANTENNA ELEMENT**

The fabricated prototype of the proposed antenna is shown in Fig.4. The measured axial ratios and  $|S_{11}|$  are consistent

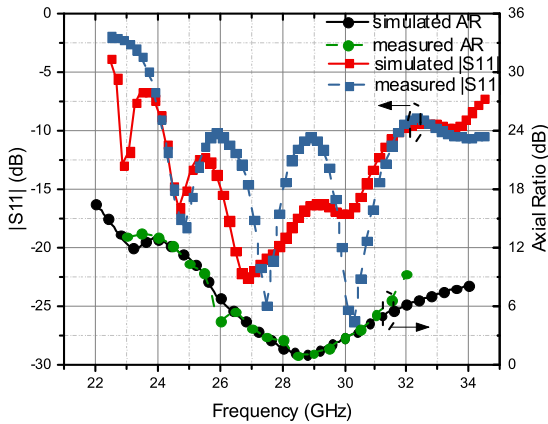


**FIGURE 5. Simulated and measured  $|S_{11}|$  and axial ratios of the proposed antenna.**

with the simulated one in Fig.5. The proposed antenna has a 3-dB AR bandwidth of 9.7% (27.4 to 30.2GHz) and a wide impedance bandwidth of 27.1% (24.29 to 31.9GHz) for  $S_{11} < -10$ dB, the reason of which is that, the electric dipole works with a resonant state, and the magnetic dipole works with a different resonant state, thus, the antenna has a wider impedance bandwidth. What’s more, compared with the conventional longitudinal slot, the bowtie-shape aperture can further expand the impedance bandwidth.

The simulated radiation patterns and measured radiation patterns at 28GHz, 29GHz and 30GHz are shown in Fig.6. The main polarization of proposed antenna is LHCP. When  $f = 29$  GHz, the LHCP is more than 20 dB higher than RHCP in the  $0^\circ$  direction of radiation pattern, which indicates the proposed antenna has a good polarization isolation. The radiation pattern of the xoz plane is similar with the radiation pattern of the yoz plane. It is noted that due to the introduction of a microstrip fed-line, the back radiation of measured radiation pattern is larger than the back radiation of simulated one. However, the measured radiation pattern is consistent with the simulated radiation pattern in terms of overall trends. Fig.7 shows simulated realized gain and measured realized gain of the proposed antenna. And the measured stable realized gain of 7.2dBic is in good agreement with the simulated one over the operating band. As shown in Fig.8, the magnitude difference of the proposed antenna is almost 0 over the operating band. However, due to the phase difference of the antenna is realized by the magnitude of chamfering and perturbation, the phase difference varies linearly with frequency over the operating band. Thus, the proposed antenna has a wide impedance bandwidth of 27.1% and a 3-dB axial-ratio bandwidth of 9.7%.

### III. DESIGN AND FABRICATION OF ANTENNA ARRAY

#### A. GEOMETRY OF 1 × 2 ANTENNA ARRAY

Fig.9 shows the geometry of the 1 × 2 antenna array. The designed antenna array includes a 1 × 2 antenna array portion and a complementary SIW power distribution phase shifter portion which includes a matching segment, a power

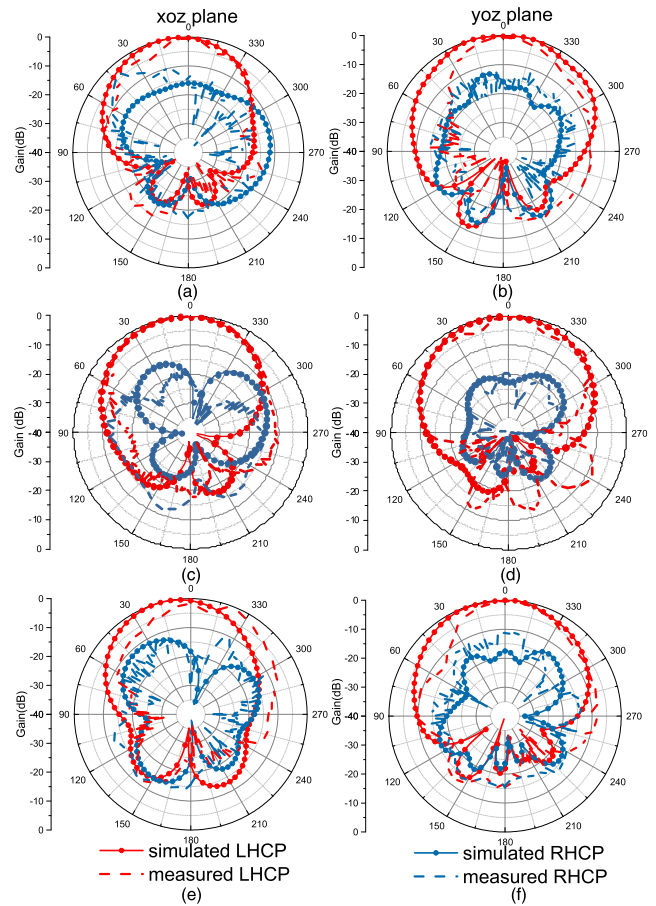


**FIGURE 6. Simulated and measured radiation patterns of the proposed antenna at 28GHz, 29GHz and 30GHz.**

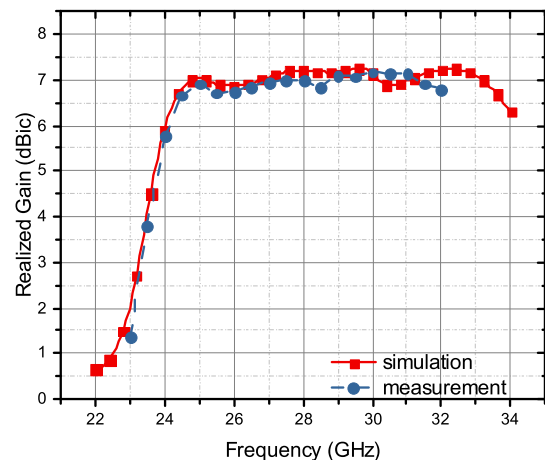


**FIGURE 7. Simulated and measured realized gain of the proposed antenna.**

distribution segment and a pair of phase shift segments. By extending the length of one of phase shift segments, which can make the phase ahead, and shortening the width of another, which can make the phase behind [24], the proposed complementary SIW power distribution phase shifter can generate two kind of electromagnetic energy, which has a stable phase difference over the operating band. In order to

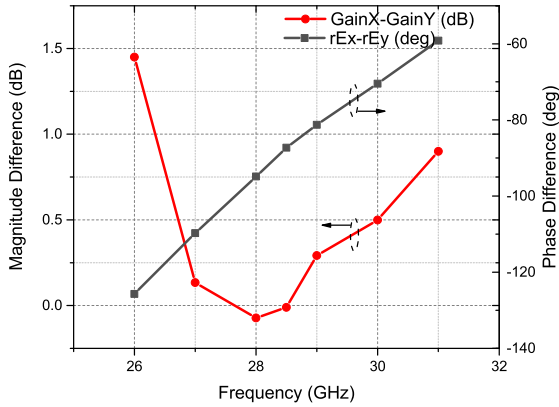


FIGURE 8. Magnitude difference and phase difference of the proposed antenna.

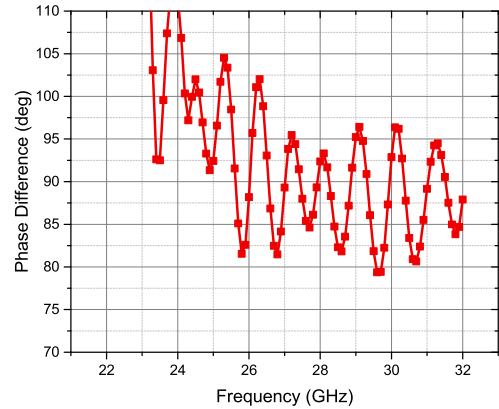


FIGURE 10. Phase difference of two output port of the proposed complementary SIW power distribution phase shifter.

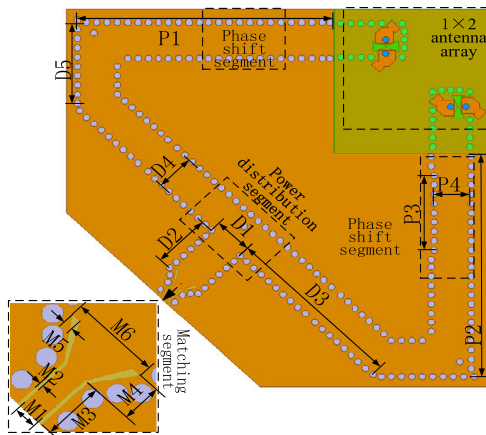


FIGURE 9. Geometry of  $1 \times 2$  antenna array.

TABLE 2. Dimensional parameters of the  $1 \times 2$  antenna array.

Parameter	M1	M2	M3	M4	M5	M6
Value(mm)	1.14	0.2	3	2	0.5	4.4
Parameter	D1	D2	D3	D4	D5	P1
Value(mm)	5.8	8.6	27.3	5.8	13	37.2
Parameter	P2	P3	P4			
Value(mm)	36	12	5.4			

facilitate the measurement, a GCPW to SIW interface is used at the front port of complementary SIW power distribution phase shifter. By using a gradient segment with length of about quarter of wavelength and an inductive triangular slot, the complementary SIW power distribution phase shifter has the low insertion loss and the wide bandwidth. Detailed dimensions of the proposed wideband CP  $1 \times 2$  antenna array is given in Table 2.

As shown in Fig.10, the phase difference of two output ports of proposed complementary SIW power distribution phase shifter is  $90^\circ \pm 10^\circ$  from 26.3 to 32GHz.  $S_{11} < -10\text{dB}$ ,  $S_{21}$  and  $S_{31} = 3.5 \pm 0.5\text{dB}$  from 24.4 to 31.6GHz in Fig.11, which confirms the power divider phase shifter provides two

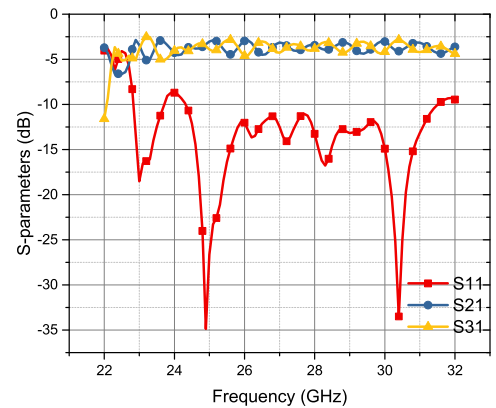
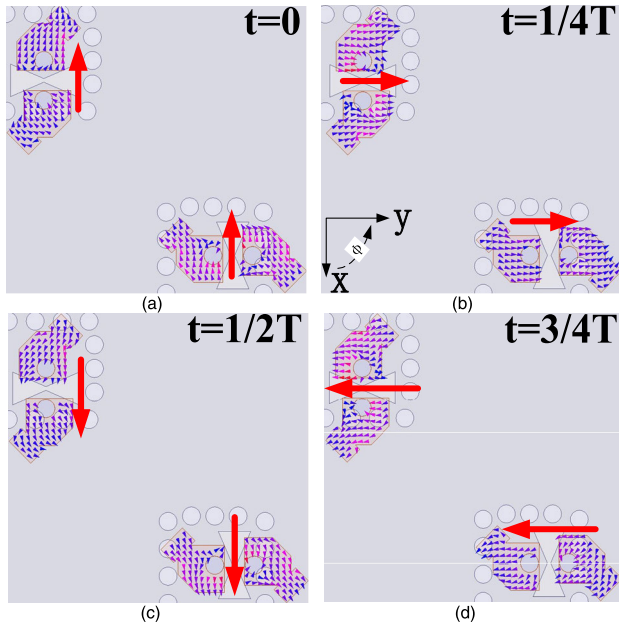


FIGURE 11. S-parameters of the proposed complementary SIW PD phase shifter.

antenna elements with two kind of electromagnetic energy which have equal magnitude and  $90^\circ$  phase difference over a wide bandwidth. Fig.12 shows simulated current distribution on proposed  $1 \times 2$  antenna array at different times  $t = 0, T/4, T/2$  and  $3T/4$ . where  $T$  is the period of oscillation when operating frequency is 28GHz. It is easy to see that the current of two antenna elements are always in the same direction. At time  $t = 0$ , the current on the surface of the proposed  $1 \times 2$  antenna array flows along the direction of  $\varphi = \pi$ . When  $t = T/4$ , the proposed  $1 \times 2$  antenna array's surface current flows along the direction of  $\varphi = \pi/2$ . As  $t = T/2$ , the current on the  $1 \times 2$  antenna array flows along the direction of  $\varphi = 0$ . As  $t = 3T/4$ , the  $1 \times 2$  antenna array's current flows along the direction of  $\varphi = -\pi/2$ . With the time varies, the current on the surface of the proposed  $1 \times 2$  antenna array rotates in the clockwise direction. Therefore, the proposed magneto-electric dipole antenna array can generate left-hand CP radiation.

### B. MEASUREMENT OF $1 \times 2$ ANTENNA ARRAY

The fabricated prototype of the proposed  $1 \times 2$  antenna array is depicted in Fig.13. Fig.14 indicates the simulated and measured  $|S_{11}|$  and AR of proposed  $1 \times 2$  antenna array. The measured  $|S_{11}|$  and axial ratios are in good agreement with simulated one. The proposed  $1 \times 2$  antenna



**FIGURE 12.** Current distribution of the proposed  $1 \times 2$  antenna array at 28 GHz. (a)  $t = 0$ , (b)  $t = T/4$ , (c)  $t = T/2$ , (d)  $t = 3T/4$ .

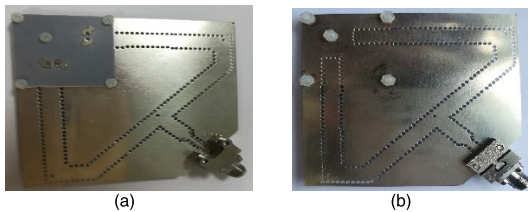


**FIGURE 13.** Photographs of the fabricated  $1 \times 2$  antenna array. (a) Top view, (b) bottom view.

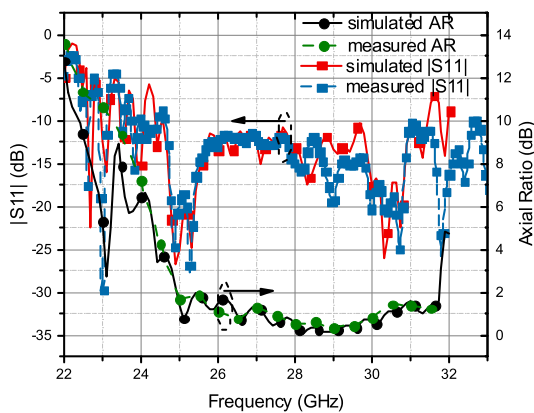


**FIGURE 14.** Simulated and measured  $|S_{11}|$  and Axial Ratios of the  $1 \times 2$  antenna array.

array has an impedance bandwidth of 25% (24.4 to 31.4GHz) for  $S_{11} < -10\text{dB}$  and a 3-dB axial-ratio bandwidth of 24.7% (24.8 to 31.7GHz), which is 2.4 times higher than the 3-dB AR bandwidth of one antenna element. Thus, the proposed antenna array realizes both broadband impedance bandwidth and broadband 3-dB AR bandwidth.

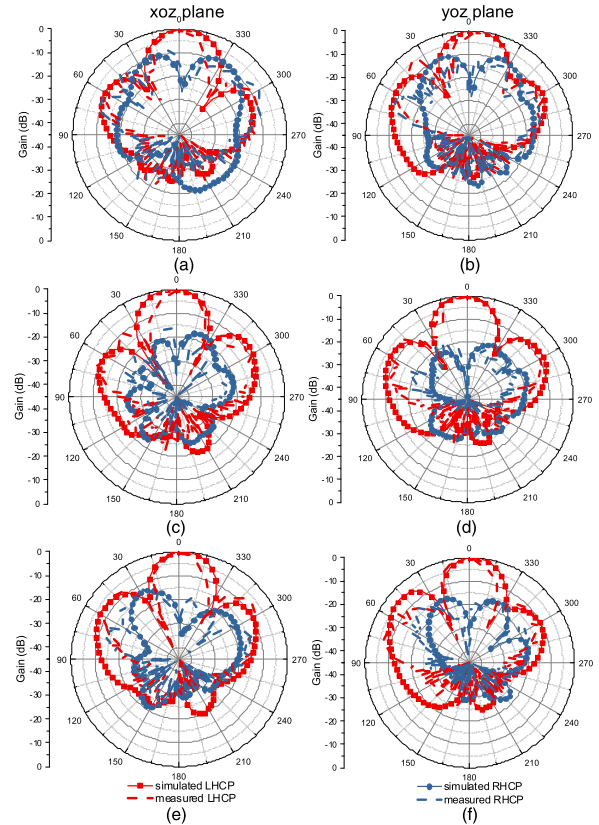


**FIGURE 15.** Simulated and measured radiation patterns of the proposed  $1 \times 2$  antenna array at 26GHz, 28GHz and 30GHz.

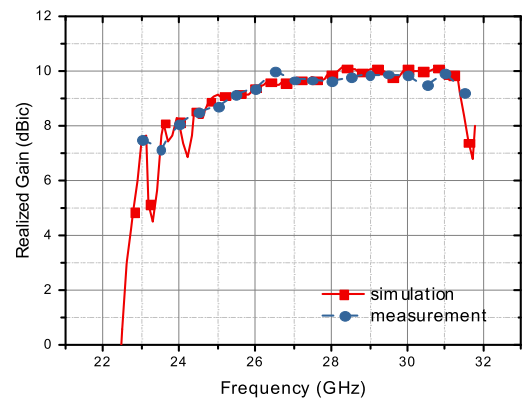


**FIGURE 16.** Simulated and measured realized gain of the proposed  $1 \times 2$  antenna array.

The simulated and measured radiation patterns at 26GHz, 28GHz and 30GHz are depicted in Fig.15. The main polarization of the proposed wideband CP  $1 \times 2$  antenna array is LHCP. And the LHCP is more than 20 dB higher than RHCP in the  $0^\circ$  direction of radiation pattern over the operating band, which indicates the  $1 \times 2$  antenna array has good polarization isolation. The radiation pattern of the xoz plane is similar with the radiation pattern of the yoz plane. It is noted that, in order to ensure the similarity of the radiation pattern of plane xoz and plane yoz, and make the  $1 \times 2$  antenna array have a good 3-dB AR bandwidth, the distance

**TABLE 3. Performance comparison with the proposed antenna.**

Ref	Center Freq. (GHz)	Geometry Features	S <sub>11</sub>   BW (%)	AR BW (%)
[9]	33	Planar PCB	26	11
[10]	11.7	Planar PCB	7.9	9
[11]	29	Planar PCB	15.45	5.4
[12]	15	Planar PCB	12.6	9
[13]	60	Planar PCB	16.1	18.8
[19]	60	Planar PCB	18.2	16.5
[20]	30	Planar PCB	52.9	41
[21]	4.8	Metallic Structure	58	28.4
[22]	95	Metallic Structure	16.8	14.5
[23]	95	Metallic Structure	16.8	17
Prop.	28	Planar PCB	25	24.7

between the antenna elements is designed with a larger value. Which will lead the sidelobe of the array is relatively large. Fig.16 shows simulated and measured realized gain of the proposed  $1 \times 2$  antenna array. The measured stable realized gain of 10dBic is in good agreement with the simulated one over the operating band. As is shown in figure 13, compared with the size of radiator, the size of the feed network looks larger. However, it is not serious. When an array with a larger size is required, the disadvantage about the feed network's large size could be solved by adopting the method of stacked patch.

#### IV. CONCLUSION

This paper presents a novel wideband CP magneto-electric dipole  $1 \times 2$  antenna array for millimeter-wave applications. Based on a novel and simple single radiator, an antenna unit is designed which has an impedance bandwidth of 27.1% for  $S_{11} < -10$ dB, an AR bandwidth of 9.7% and a stable gain of 7dBic. The proposed  $1 \times 2$  antenna array is fed by a complementary SIW power distribution phase shifter and has an wide impedance bandwidth of 25% for  $S_{11} < -10$ dB from 24.4 to 31.4GHz, a stable gain of 10dBic and an axial-ratio bandwidth of 24.7% for  $AR < 3$ dB from 24.8 to 31.7GHz, which is 2.4 times higher than the 3-dB AR bandwidth of a single radiator. Moreover, the proposed  $1 \times 2$  antenna array has good polarization isolation in the operating band, and the radiation pattern of the xoz plane is similar with that of the yoz plane.

#### REFERENCES

- [1] F. Ferrero, C. Luxey, G. Jacquemod, and R. Staraj, "Dual-band circularly polarized microstrip antenna for satellite applications," *IEEE Antennas Wireless Propag. Lett.*, vol. 4, pp. 13–15, 2005.
- [2] J.-S. Row and S.-W. Wu, "Circularly-polarized wide slot antenna loaded with a parasitic patch," *IEEE Trans. Antennas Propag.*, vol. 56, no. 9, pp. 2826–2832, Sep. 2008.
- [3] S. X. Ta, I. Park, and R. W. Ziolkowski, "Circularly polarized crossed dipole on an HIS for 2.4/5.2/5.8-GHz WLAN applications," *IEEE Antennas Wireless Propag. Lett.*, vol. 12, pp. 1464–1467, 2013.
- [4] B. A. Zeb, N. Nikolic, and K. P. Esselle, "A high-gain dual-band EBG resonator antenna with circular polarization," *IEEE Antennas Wireless Propag. Lett.*, vol. 14, pp. 108–111, 2015.
- [5] R. Xu, J.-Y. Li, and W. Kun, "A broadband circularly polarized crossed-dipole antenna," *IEEE Trans. Antennas Propag.*, vol. 64, no. 10, pp. 4509–4513, Oct. 2016.
- [6] P. Sharma and K. Gupta, "Analysis and optimized design of single feed circularly polarized microstrip antennas," *IEEE Trans. Antennas Propag.*, vol. 31, no. 6, pp. 949–955, Nov. 1983.
- [7] A. B. Guntupalli and K. Wu, "60-GHz circularly polarized antenna array made in low-cost fabrication process," *IEEE Antennas Wireless Propag. Lett.*, vol. 13, pp. 864–867, 2014.
- [8] Y. Cai, Y. Zhang, Z. Qian, W. Cao, and S. Shi, "Compact wide-band dual circularly polarized substrate integrated waveguide horn antenna," *IEEE Trans. Antennas Propag.*, vol. 64, no. 7, pp. 3184–3189, Jul. 2016.
- [9] W. Han, F. Yang, J. Ouyang, and P. Yang, "Low-cost wideband and high-gain slotted cavity antenna using high-order modes for millimeter-wave application," *IEEE Trans. Antennas Propag.*, vol. 63, no. 11, pp. 4624–4631, Nov. 2015.
- [10] T. Hong, S. Wang, Z. Liu, and S. Gong, "RCS reduction and gain enhancement for the circularly polarized array by polarization conversion metasurface coating," *IEEE Antennas Wireless Propag. Lett.*, vol. 18, no. 1, pp. 167–171, Jan. 2019.
- [11] A. Chen, Y. Zhang, Z. Chen, and S. Cao, "A Ka-band high-gain circularly polarized microstrip antenna array," *IEEE Antennas Wireless Propag. Lett.*, vol. 9, pp. 1115–1118, 2010.
- [12] R. Orr, G. Goussetis, and V. Fusco, "Design method for circularly polarized Fabry–Pérot cavity antennas," *IEEE Trans. Antennas Propag.*, vol. 62, no. 1, pp. 19–26, Oct. 2013.
- [13] J. Zhu, S. Liao, S. Li, and Q. Xue, "60 GHz wideband high-gain circularly polarized antenna array with substrate integrated cavity excitation," *IEEE Antennas Wireless Propag. Lett.*, vol. 17, no. 5, pp. 751–755, May 2018.
- [14] H. Oraizi and R. Pazoki, "Wideband circularly polarized aperture-fed rotated stacked patch antenna," *IEEE Trans. Antennas Propag.*, vol. 61, no. 3, pp. 1048–1054, Mar. 2013.
- [15] J. Wu, Y. Yin, Z. Wang, and R. Lian, "Broadband circularly polarized patch antenna with parasitic strips," *IEEE Antennas Wireless Propag. Lett.*, vol. 14, pp. 559–562, 2015.
- [16] S. Fu, Q. Kong, S. Fang, and Z. Wang, "Broadband circularly polarized microstrip antenna with coplanar parasitic ring slot patch for L-band satellite system application," *IEEE Antennas Wireless Propag. Lett.*, vol. 13, pp. 943–946, 2014.
- [17] M. Li and K.-M. Luk, "Low-cost wideband microstrip antenna array for 60-GHz applications," *IEEE Trans. Antennas Propag.*, vol. 62, no. 6, pp. 3012–3018, Jun. 2014.
- [18] H. Sun, Y.-X. Guo, and Z. Wang, "60-GHz circularly polarized U-slot patch antenna array on LTCC," *IEEE Trans. Antennas Propag.*, vol. 61, no. 1, pp. 430–435, Jan. 2013.
- [19] Y. Li and K.-M. Luk, "A 60-GHz wideband circularly polarized aperture-coupled magneto-electric dipole antenna array," *IEEE Trans. Antennas Propag.*, vol. 64, no. 4, pp. 1325–1333, Apr. 2016.
- [20] J. Wang, Y. Li, L. Ge, J. Wang, M. Chen, Z. Zhang, and Z. Li, "Millimeter-wave wideband circularly polarized planar complementary source antenna with endfire radiation," *IEEE Trans. Antennas Propag.*, vol. 66, no. 7, pp. 3317–3326, Jul. 2018.
- [21] J. Sun and K.-M. Luk, "Wideband linearly-polarized and circularly-polarized aperture-coupled magneto-electric dipole antennas fed by microstrip line with electromagnetic bandgap surface," *IEEE Access*, vol. 7, pp. 43084–43091, 2019.
- [22] J. Cao, H. Wang, S. Mou, S. Quan, and Z. Ye, "W-band high-gain circularly polarized aperture-coupled magneto-electric dipole antenna array with gap waveguide feed network," *IEEE Antennas Wireless Propag. Lett.*, vol. 16, pp. 2155–2158, 2017.
- [23] J. Cao, H. Wang, S. Mou, P. Sothar, and J. Zhou, "An air cavity-fed circularly polarized magneto-electric dipole antenna array with gap waveguide technology for mm-wave applications," *IEEE Trans. Antennas Propag.*, vol. 67, no. 9, pp. 6211–6216, Sep. 2019.
- [24] Y. Jian Cheng, W. Hong, and K. Wu, "Broadband self-compensating phase shifter combining delay line and equal-length unequal-width phaser," *IEEE Trans. Microw. Theory Techn.*, vol. 58, no. 1, pp. 203–210, Jan. 2010.



**YING-FANG WANG** was born in Jiaozuo, Henan, China, in 1994. He received the bachelor's degree in electronic information engineering from Henan Polytechnic University, Jiaozuo, China, in 2017. He is currently pursuing the master's degree with the National Key Laboratory of Antennas and Microwave Technology, Xidian University.

His research interests include circularly polarized antenna, electromagnetic compatibility, and microwave passive and active circuits.



**BIAN WU** (Member, IEEE) was born in Xianning, Hubei, China, in 1981. He received the B.S. and Ph.D. degrees in electromagnetic fields and microwave technology from Xidian University, Xi'an, China, in 2004 and 2008, respectively.

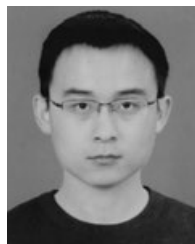
Since 2008, he has been with Xidian University, where he is currently a Professor and a Ph.D. Supervisor with the National Key Laboratory of Antennas and Microwave Technology. From March 2013 to February 2014, he was a

Postdoctoral Visitor with the Queen Mary University of London, U.K. He has authored or coauthored over 80 journal publications. His research interests include microwave circuits and devices, filtering antennas, metamaterials, and graphene-based devices.



**NAN ZHANG** was born in Chaoyang, Liaoning, China, in 1991. He received the bachelor's and master's degrees in electromagnetic fields and microwave technology from Xidian University, Xi'an, China, in 2014 and 2019, respectively.

He is currently working with the RF Research and Development Department, ZTE China. His research interests include circularly polarized antenna, magneto-electric dipole, and antenna for millimeter waves.



**YU-TONG ZHAO** was born in Tongchuan, Shaanxi, China, in 1991. He received the B.S. and Ph.D. degrees in electromagnetic fields and microwave technology from Xidian University, Xi'an, China, in 2013 and 2018, respectively.

Since 2019, he has been with Xidian University, where he currently holds a postdoctoral position with the National Key Laboratory of Antennas and Microwave Technology. His research interests include microwave circuits and devices, filtering

antennas, metamaterials, and graphene-based devices.



**TAO SU** was born in Jinan, Shandong, China, in 1974. He received the B.S., M.E., and Ph.D. degrees in electromagnetic field and microwave technology from Xidian University, Xi'an, China, in 1997, 2000, and 2004, respectively.

In 2004, he joined the School of Electronic Engineering, Xidian University, Xi'an, where he is currently a Full Professor and the Associate Dean with the National Key Laboratory of Antennas and Microwave Technology. His research interests

include microwave circuits and systems, RF/microwave filters and antennas, and electromagnetic compatibility.

...